Biodegradable ionic liquids as lubricants

Nicklas Hjalmarsson[1)*], Rubén Álvarez Asencio[1)], James Sweeney[2)], Faiz U. Shah[3)], Fredrik Schaufelberger[4)], Olof Ramström[4)], Oleg N. Antzutkin[3,5)], Rob Atkin[2,4)], Sergei Glavatskih[5)], and Mark W. Rutland[1,6)]

[1)] Surface and Corrosion Science, School of Chemical Science and Engineering,
KTH – Royal Institute of Technology, Stockholm, Sweden
[2)] Centre for Advanced Particle Processing and Transport, University of Newcastle, Callaghan, NSW, Australia
[3)] Chemistry of Interfaces, Luleå University of Technology, Luleå, Sweden
[4)] Organic Chemistry, School of Chemical Science and Engineering,
KTH – Royal Institute of Technology, Stockholm, Sweden
[5)] Department of Physics, The University of Warwick, Coventry, UK
[4)] Centre for Organic Electronics, University of Newcastle, Callaghan, NSW, Australia
[5)] System and Component Design, School of Industrial Engineering and Management,
KTH – Royal Institute of Technology, Stockholm, Sweden
[6)] SP – Chemistry, Materials, and Surfaces, Stockholm, Sweden
*Corresponding author: nhja@kth.se

1. Introduction

The use of lubricants is one way of minimizing heat loss in a system since they reduce friction by keeping moving parts apart, transfer heat, act as carriers, and prevent corrosion. However, most of the lubricants currently used degrade at higher temperatures, and are often not environmentally friendly. They were developed for ferrous materials. Today, the trend is towards using non-ferrous metal alloys and wear resistant coatings. Therefore, it is necessary to find compatible lubricants that are also biodegradable.

Ionic liquids (ILs) present a potential answer to the need for new and more tunable lubricants. They are defined as salts existing in their liquid form below 100°C. ILs are generally thermally and electrochemically very stable, have high viscosities, high conductivities, and low vapor pressures. There are potentially up to 10^{18} different ILs, so the possibility of tuning to a specific task is high. Recent published articles indicate that the investigated ILs have good tribological properties both on a micro- and nanoscale [1, 2]. Furthermore, in one of the articles it was also shown that the interfacial viscosity is considerably lower than the bulk value for ethylammonium nitrate (EAN) at room temperature [3].

Current work focuses on how ILs behave at temperatures higher than the ambient temperature normally used in Atomic Force Microscopy (AFM) measurements. We use Colloidal Probe AFM to immerse ILs between a silica sphere and a mica surface to investigate different phenomena related to this confinement: such as, normal and friction forces and interfacial viscosity. This is done with both traditional ILs, like EAN (Figure 1), and more recently discovered ILs, for example oligoether carboxylates, like sodium 2,5,8,11-tetraoxatridecan-13-oate[Na][TOTO] [4] (Figure 2) and other halogen-free ILs [1], e.g. Trihexyltetradecylphosphonium bis(oxalate)borate [P6,6,6,14][BOB] (Figure 3).

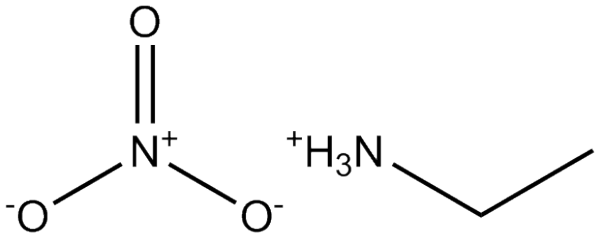

Figure 1. Ethylammonium nitrate (EAN)

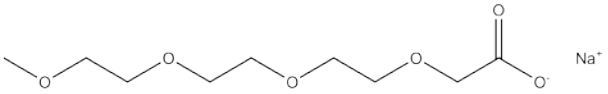

Figure 2. Sodium 2,5,8,11-tetraoxatridecan-13-oate[Na][TOTO]

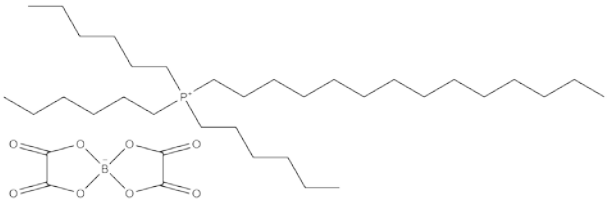

Figure 3. Trihexyltetradecylphosphonium bis(oxalate)borate [$P_{6,6,6,14}$][BOB]

Force and friction measurements for EAN display lower friction at higher temperature, with maintained, although weakened, structural ordering at the tribological interface, compared to room temperature. The interfacial viscosity is also lower than the bulk viscosity at higher temperatures, following the same trend as Álvarez Asencio *et al.* demonstrated [3]. Initial experiments done with [$P_{6,6,6,14}$][BOB] at high temperatures also reveals interesting characteristics. [Na][TOTO] has at the time of writing been synthesized but not yet investigated.

2. Results and Discussion

The results presented here are only intended to give a brief overview of achievements so far.

2.1 Interfacial ordering

Atkin *et al.* previously demonstrated the structure of a number of ILs under confinement [5]. In the paper several discrete steps could be observed in the force curves. These steps were explained as the AFM-tip penetrating through a layer of IL. For EAN it was shown that the steps were consistent with the diameter of an EAN ionic pair which has been determined to be 0.5 nm. As the tip is moving through the layers it will experience a greater force as it gets closer to the surface due to increased ordering. However, previous publications suggest that these layers will rupture at higher temperature due to thermal motion [6].

The force curves, shown in Figure 4, for EAN demonstrate that steps, previously seen for EAN only at and around room temperature and very low speeds, could be distinguished independent of speed at much higher speeds and temperatures, it was also shown that the interfacial viscosity is much lower than the bulk value. Normally, fluiddynamic forces would convolute the interaction between probe and surface; this would be manifested as a rate dependence in the force curve and has been shown to exist for EAN at room temperature [3].

This experiment reveals that another mechanism is working in parallel, indicating that the high viscosity of EAN screens the steps at low temperatures/high speeds and that the effect thermal motion has on the layering of EAN is less than previously thought. As the temperature is increased, viscosity is decreased and at sufficiently high temperature the interfacial viscosity has reached a level low enough for our experimental setup to detect the steps, even at "high" approach speeds. This indicates that at least some of the boundary properties are retained, even when the viscosity is low.

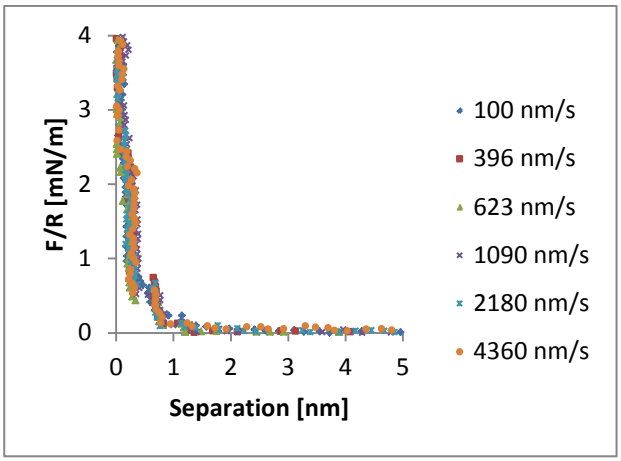

Figure 4. Force curve obtained at 75 °C and six different speeds for EAN.

2.2 Friction

Figure 5 follows on with the same reasoning as in ***2.1*** and demonstrates regions with different frictional behavior depending on the amount of force applied to the system. Especially the breaking point, happening at an applied load of approximately 20 nN, is interesting and indicates that the transition into the final sliding regime is temperature dependent.

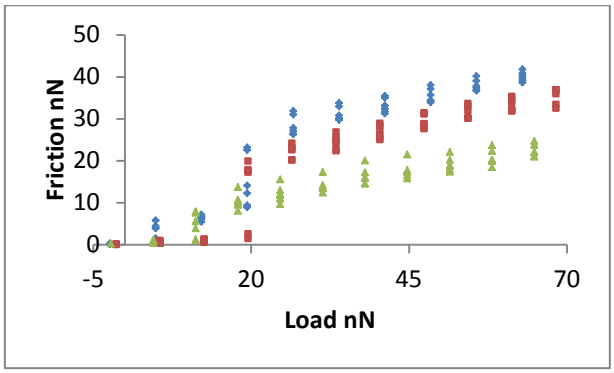

Figure 5. Friction loop showing temperature dependence for EAN at a speed of 10 µm/s. The blue diamonds show measurements done at room temperature, the red squares were done at 45 °C, and the green triangles at 75 °C.

3. Methods and Materials

All the water used throughout the experiments was purified to a resistivity of 18.2 MΩ cm employing a Milli-Q Purification System (Millipore, Malsheim, France).

3.1 EAN and [$P_{6,6,6,14}$][BOB]

Ethylammonium nitrate (EAN) was synthesized by drop-wise addition of concentrated nitric acid to a solution of ethylamine, under constant agitation, until equimolar amounts was mixed. This was done with excess water and the system was cooled to a temperature below 10 °C with ice during the reaction stage to prevent oxide formation. The solution was then subject to rotary evaporation at 50 °C for 2 h after completed reaction to remove water left. However, this treatment did not completely remove all water from the solution and it was therefore purged with nitrogen and heated to 110 °C overnight under a nitrogen atmosphere. [$P_{6,6,6,14}$][BOB] was received as a gift from collaborators and was synthesized according to the details found in the supplementary material from Shah *et al.* [1].

3.2 [Na][TOTO]

The target molecule was synthesized according to a two-step modified literature procedure [4], where the acid of the oligoether carboxylate was first synthesized before the final product was obtained.

2,5,8,11-Tetraoxatridecan-13-oic acid [TOTOA]

Sodium metal (2.19 g, 95.4 mmol) was added portion-wise over 1 h at room temperature to vigorously stirred neat triethylene glycol monomethyl ether (26 ml, 26.7 g, 162 mmol) in a dry two-necked round bottom flask

under N_2. After addition of the reagent, the heterogenous mixture was heated to 120 °C and stirred until complete dissolution of the sodium (ca 3 h). A light flow of N_2 was applied in the system to drive away H_2 gas that formed. Afterwards, the reaction mixture was cooled to 100 °C, and chloroacetic acid (4.53 g, 47.7 mmol) dissolved in triethylene glycol monomethyl ether (10 ml, 10.3 g, 62.5 mmol) was added drop-wise. The resulting milky heterogenous mixture was stirred at 100 °C under N_2 for 12 h. Upon completion of the reaction (monitored by NMR), excess triethylene glycol monomethyl ether was carefully distilled off (p = 2.1 mmHg, bp = 96-98 °C), leaving a brown suspension. After cooling to room temperature, 1 M solution of HCl (75 ml) was slowly added under stirring, and the yellow aqueous solution was extracted with CH_2Cl_2, (4 x 70 ml).

Further purification of the almost pure product mixture was performed by saponification of the acid. The organic phase was concentrated *in vacuo*, and then sat. aq. $NaHCO_3$ solution was slowly added to the resulting oil until TLC analysis showed complete deprotonation of the acid. CH_2Cl_2 (3 vol. eq.) was then added, and the phases were separated. The aqueous phase was acidified by drop-wise addition of 1 M aq. HCl solution at 0 °C until pH <4. Finally, the aqueous phase was repeatedly extracted with CH_2Cl_2, and the organic phase was dried with $MgSO_4$, filtered and concentrated to yield the analytically pure product as a colorless oil (26.2 mmol, 55% yield).

^{1}H-NMR (500 MHz, $CDCl_3$) δ 9.91 (s, br, 1H, -*COOH*), 4.16 (s, 2H, O-*CH_2*-COOH), 3.59-3.61 (m, 2H, -*CH2*-), 3.66-3.72 (m, 8H, -*CH2*-), 3.78-3.80 (m, 2H, -*CH2*-), 3.39 (s, 3H, *H_3C*-O);

Sodium 2,5,8,11-tetraoxatridecan-13-oate [Na][TOTO]

TOTOA (3.18 g, 14.3 mmol) was weighed up in a round bottom flask and dissolved in H_2O. To this, $NaHCO_3$ (1.20 g, 14.3 mmol) was added portion-wise and the resulting solution was stirred for 1 h at room temperature. The water was removed by lyophilization, followed by brief drying under reduced pressure at 120 °C, yielding the highly viscous ionic liquid product in quantitative yield. ^{1}H NMR spectroscopic data was consistent with previously reported data [4].

^{1}H-NMR (500 MHz, $CDCl_3$) δ 3.89 (s, 2H, O-*CH_2*-COO^-), 3.56-3.69 (m, 12H, -*CH2*-), 3.39 (s, 3H, *H_3C*-O);

3.3 Cleaning procedures

All material used was thoroughly cleaned prior to experiments. The AFM liquid cell and O-ring was rinsed with copious amounts of water, followed by ethanol of highest purity (99.9 %, Kemetyl, Haninge Sweden), and then dried with nitrogen. Tubing, connectors, tweezers and other accessories were always stored in a glass beaker containing 70 % ethanol and ultrasonicated for at least 30 minutes and there after treated the same way as the liquid cell and the O-ring prior to use. The cantilever used for carrying out the experiment was cleaned in the same way as the liquid cell and the O-ring, but upon completion of that cleaning stage it was also subject to plasma treatment for 15 s.

3.4 Particle attachment and cantilever calibration

A silica particle was attached (Bangs Laboratories, Fishers, IN, USA) to a tipless cantilever (CSC12, Mikromasch, Tallinn, Estonia) using Araldite^{TM} epoxy glue (Hunstman LLC, Duxford, United Kingdom) under an optical microscope, connected to a micromanipulator to allow fine adjustment of the colloid particle. The particle radius, length and width of the cantilever and other dimensions needed were obtained using ImageJ software (NIST, Gaithersburg, MD, USA). These values were then used to calculate the normal spring constant by following Sader's method of thermal vibration [7]. The torsional spring constant was determined using the following equation together with the acquired cantilever dimensions:

$$k_T = \frac{k_N 4L^3}{6(1+\nu)(L-\Delta L)}\left[1-\left(\frac{\tanh\left(\frac{L-\Delta L}{w}\sqrt{6(1-\nu)}\right)}{\sqrt{6(1-\nu)}}\frac{w}{(L-\Delta L)}\right)\right]^{-1} \quad (1)$$

where L and w are the length and the width of the cantilever, ΔL is the distance from the cantilever's free end to the center of the probe used, and ν is Poisson's ratio. The mica surfaces used were freshly cleaved prior to experiments.

3.5 Force and Friction experiments

All normal force and friction measurements were performed using a Nanoscope IIIa Multimode AFM (Bruker, Santa Barbara, CA, USA) equipped with a PicoForce scanner in contact mode and a PicoForce controller. The normal force curves were obtained using a ramp size of 100 nm at a scan rate of 0.015 Hz with a maximum deflection of 2 V and a 1 s surface delay to detect steps on retraction. The data recorded by the AFM are deflection of the cantilever against the separation. These were then converted to force as a function of apparent separation using the ForceIT v.2.6.1 software (ForceIT, Sweden) and approximating zero separation as the region of constant compliance. A total of 25 curves were obtained. For friction a scan size of 5 μm was used (512 points/line, 32 lines) with five different scan rates (0.5, 1, 2, 3, and 4 Hz) to allow for velocity dependence as well as friction as a function of load. The applied load was increased from 0 to 2 V, and then unloaded to -0.2 V, with a constant increment of 0.2 V. The friction coefficient can be determined as the slope when plotting the friction force against the applied load, provided the relationship is linear [8].

4. References

[1] Shah, F. U., Glavatskih, S., Macfarlane, D. R., Somers, A., Forsyth, M. & Antzutkin, O. N., "Novel halogen-free chelated orthoborate-phosphonium ionic liquids: synthesis and tribophysical properties", Physical Chemistry Chemical Physics, 13**,** 2011, 12865-12873.

[2] Sweeney, J., Hausen, F., Hayes, R., Webber, G. B., Endres, F., Rutland, M. W., Bennewitz, R., Atkin, R., "Control of Nanoscale Friction on Gold in an Ionic Liquid by a Potential-Dependent Ionic Lubricant Layer", Physical Review Letters, 109, 2012, 155502.

[3] Álvarez Asencio, R., Cranston, E. D., Atkin, R. & Rutland, M. W., "Ionic Liquid Nanotribology: Stiction Suppression and Surface Induced Shear Thinning", Langmuir, 28**,** 2012, 9967-9976.

[4] Zech, O., Kellermeir, M., Thomaier, S., Maurer, E., Klein, R., Schreiner, C., Kunz, W., "Alkali Metal Oligoether Carboxylates - A New Class of Ionic Liquids", Chemistry - a European Journal, 15, 2009, 1341-1345.

[5] Atkin, R., Warr, G. G., "Structure in Confined Room-Temperature Ionic Liquids", Journal of Physical Chemistry C, 111, 2007, 5162-5168.

[6] Wakeham, D., Hayes, R., Warr, G. G., Atkin, R., "Influence of Temperature and Molecular Structure on Ionic Liquid Solvation Layers", Journal of Physical Chemistry B, 113, 2009, 5961-5966.

[7] Sader, J. E., Chon, J. W. M., Mulvaney, P., "Calibration of Rectangular Atomic Force Microscope Cantilvers", Review of Scientific Instruments, 70, 1999, 3967-3969.

[8] Amontons, G., "De la résistance causée dans les Machines", Mémoires de l'Académie Royale A, 1699, 257-282.